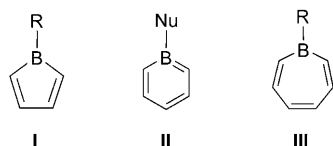


# Benzo- and Naphthoborepins: Blue-Emitting Boron Analogues of Higher Acenes\*\*

Lauren G. Mercier, Warren E. Piers,\* and Masood Parvez

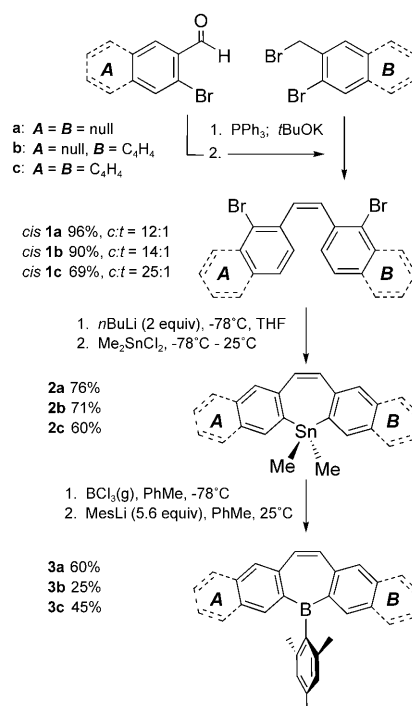
Unsaturated rings containing boron have been of fundamental and practical interest for many years.<sup>[1]</sup> Five-membered borole rings **I** are isoelectronic to the antiaromatic cyclopentadienyl cation and have been important in addressing concepts of aromaticity.<sup>[2]</sup> The six-membered borabenzene and boratabenzene compounds **II** (Nu = nucleophile),<sup>[3]</sup> however, are aromatic and have found application as cyclopentadienide-like ligands with substantial tunability at the boron substituent.<sup>[4]</sup> More recently, these cores have been tested as organic materials, finding application as fluoride sensors.<sup>[5]</sup>



The seven-membered borepin framework **III** is by comparison less explored, even though it is an aromatic six- $\pi$ -electron system, isoelectronic to the tropylium ion.<sup>[6]</sup> This paucity of information is in part due to the lack of general synthetic routes to this functionality, but the tendency of the unsupported borepin ring to undergo thermal transformations is also problematic.<sup>[7]</sup> For the latter reason, those borepins that are known tend to be annulated by other rings,<sup>[8]</sup> which provides a stabilizing influence on the borepin core structure.<sup>[9]</sup>

We have been interested in boron-containing analogues of higher acenes,<sup>[10]</sup> given the utility of the all-carbon species in organic semiconductor applications.<sup>[11]</sup> Accordingly, we have prepared dibenzoborepin, benzonaphthoborepin, and dinaphthoborepin derivatives incorporating a B-mesityl group as analogues of anthracene, tetracene, and pentacene, respectively.

The route developed is shown in Scheme 1 and relies on a tin–boron exchange reaction that has been applied with wide success in other synthetic protocols for boron heterocycles. In



**Scheme 1.** Synthesis of B-mesityl annulated borepins **3a–c**.

the first step, a Wittig reaction is utilized to prepare the *cis*-dibromo diaryl ethylenes **1a–c** from the appropriate *ortho*-bromo aryl aldehyde and the *ortho*-bromo benzyl bromide partners in excellent yield and high *cis:trans* (c:t) selectivity.<sup>[12]</sup> Closure to compounds **2a–c**, featuring the seven-membered stannacycle, was accomplished in variable yield by lithiating at low temperature and quenching the resulting dianionic species with Me<sub>2</sub>SnCl<sub>2</sub>; attempts at direct quenching with boron reagents such as MesB(OMe)<sub>2</sub><sup>[13]</sup> were not successful. Nevertheless, stannepins **2** were readily converted to the targeted borepins **3a–c** using an excess of BCl<sub>3</sub> and subsequent treatment with MesLi without isolation of the highly moisture-sensitive borepin chloride.<sup>[5a]</sup> The mesityl borepins were stable enough towards air and adventitious moisture to be handled in the ambient atmosphere and purified by column chromatography, but over the course of several hours, they did react with water to form B–O–B borinic esters.

NMR spectroscopic data for compounds **3** are consistent with their formulation as shown in Scheme 1. The olefinic protons in the isolated double bond of the borepin ring appear as a singlet for **3a** and **3c** at 6.80 and 6.99 ppm, respectively, in the <sup>1</sup>H NMR spectra; these protons resonate as two doublets (7.41 and 7.20, <sup>3</sup>J<sub>HH</sub> = 12.8 Hz) for the asymmetrical compound **3b**. The <sup>11</sup>B NMR spectra feature signals characteristic

[\*] L. G. Mercier, W. E. Piers, M. Parvez  
Department of Chemistry, University of Calgary  
2500 University Drive N.W., Calgary, AB, T2N 1N4 (Canada)  
Fax: (+1) 403-289-9488  
<http://www.chem.ucalgary.ca/research/groups/wpiers/>  
E-mail: wpiers@ucalgary.ca

[\*\*] Funding for this work was provided by NSERC of Canada and the Xerox Research Foundation.

Supporting information for this article is available on the WWW under <http://dx.doi.org/10.1002/ange.200902803>.

of three-coordinate, neutral boron nuclei<sup>[14]</sup> at 64.3, 67.7, and 66.7 ppm for **3a–c**, respectively.<sup>[15]</sup>

While the spectroscopic data are consistent with planar structures, X-ray crystallographic analysis<sup>[16]</sup> of each compound reveals bowed geometries; this deformation is likely due to packing effects (see below) rather than a ground-state preference for this geometry. Figure 1 shows the molecular structures of **3b** and **3c**, while Figure 2 illustrates key intermolecular packing interactions; **3a**<sup>[15]</sup> is similar to **3c** and will not be discussed in detail.

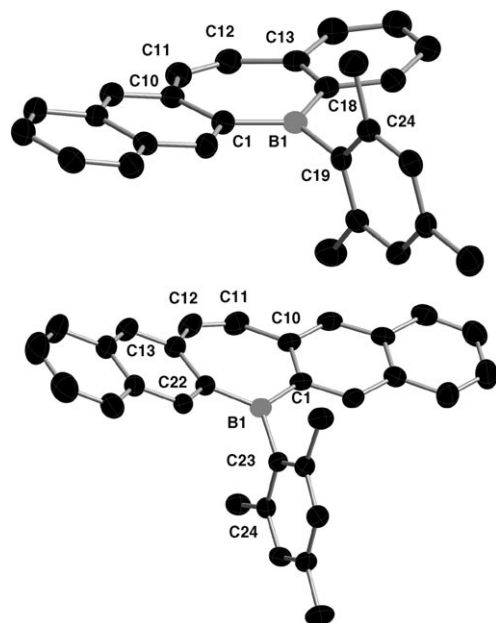


**Figure 1.** Thermal ellipsoid (50%) diagrams of the molecular structures of **3b** (top) and **3c** (bottom). Selected bond lengths [Å], angles, and dihedral angle [°] for **3b**: C1–B1 1.568(3), C1–C10 1.449(3), C10–C11 1.449(3), C11–C12 1.346(3), C12–C13 1.455(3), C13–C18 1.426(3), C18–B1 1.561(3), B1–C19 1.587(3); C1–B1–C18 126.33(19), C18–B1–C19 116.49(18), C1–B1–C19 117.10(19); C1–B1–C19–C24 88.1(3). Selected bond lengths [Å], angles, and dihedral angle [°] for **3c**: C1–B1 1.559(3), C1–C10 1.440(3), C10–C11 1.457(3), C11–C12 1.338(3), C12–C13 1.451(3), C13–C22 1.446(3), C22–B1 1.566(3), B1–C23 1.587(3), C1–B1–C22 125.98(18), C22–B1–C23 117.23(19), C1–B1–C23 116.79(18); C1–B1–C23–C24 91.4(2).

The borepin rings in each compound exhibit similar metrical properties. Intraring B–C bond lengths are approximately 0.02 Å shorter than the values for the B–C<sub>Mes</sub> bonds, indicating a degree of conjugation through the boron center in the borepin core. The C11–C12 bond gets progressively shorter for **3a** (1.386(3) Å), **3b** (1.346(3) Å), and **3c** (1.338(3) Å) and indicates a strongly localized C=C bond. The sum of the angles around the boron center is close 360° for all three compounds, with the internal angle of the seven-membered ring 7–9° larger than the others; the mesityl group is oriented essentially perpendicular to the boron trigonal plane.

Packing motifs in this series of acene analogues vary with the symmetry of the wingspan (Figure 2). In symmetrical

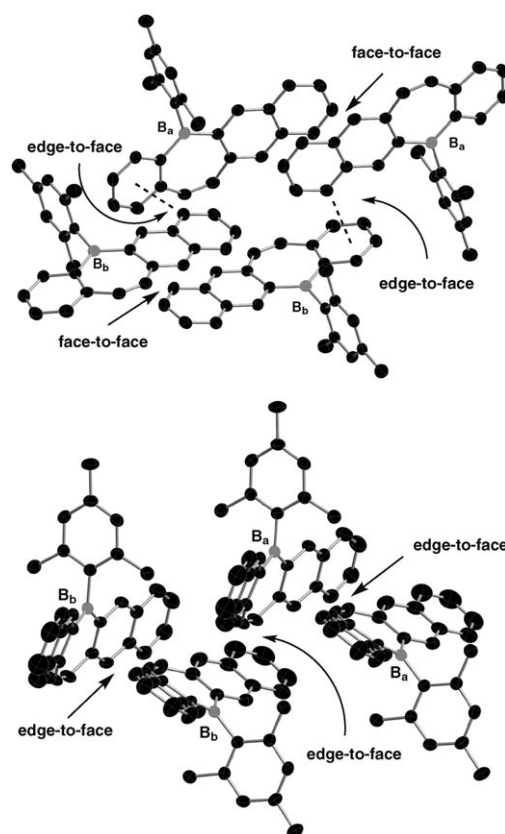


**Figure 2.** Thermal ellipsoid (50%) diagrams showing packing motifs in **3b** (top) and **3c** (bottom). In **3b**, the faces of the naphthyl moieties are approximately 3.5 Å apart in the B<sub>a</sub> and B<sub>b</sub> dimers; these units are approximately orthogonal and connected through edge-to-face interactions. In **3c** (similar to **3a**, see the Supporting Information), molecules pack in an edge-to-face herringbone motif.

compounds **3a** and **3c**, the curvature of the carbon spine engendered by the seven-membered central ring causes a bowing of the rings from planarity as a consequence of edge-to-face interactions in the herringbone packing pattern.<sup>[11]</sup> In **3c**, close interactions between C11 and C12 of one molecule with C1 and C18 of an adjacent molecule (3.6–3.8 Å) anchor this motif along the entire length of the ring system. As computations indicate that **3a–c** have planar ground-state structures (see below), these packing effects are enough to compensate for the energy required to bend the molecule from planarity. Notably, <sup>1</sup>H NMR spectra for **3a** are temperature-invariant to 223 K.

In the asymmetric heterotetracene **3b**, the primary packing interaction is a face-to-face motif<sup>[11]</sup> between the two naphthyl groups of adjacent molecules (separation ca. 3.5 Å). These face-to-face dimers pack orthogonally such that an interaction between the edge of a naphthyl group and the face of a phenyl group in an adjacent dimer can be attained. The asymmetry of this molecule may be an exploitable molecular design principle to favor face-to-face over edge-to-face interactions in heteroacenes.

Annulated borepins **3** are weaker Lewis acids than related acyclic boranes not constrained in the aromatic borepin ring. A competition experiment between **3a** and Ph<sub>2</sub>BMes reveals

that dimethylamino pyridine preferentially binds to  $\text{Ph}_2\text{BMes}$ .<sup>[15]</sup> This preference is likely due to a combination of lower availability of the empty p orbital on boron by virtue of its conjugation with the extended  $\pi$  system and the steric constraints inherent to the boron center rigidly held in the borepin ring. Accordingly, compounds **3** do not strongly bind donor solvents such as THF or diethylether. Electrochemical measurements<sup>[15]</sup> reveal reduction potentials of  $-2.56$ ,  $-2.25$ , and  $-2.20$  V for **3a–c**, relative to  $\text{Fc}/\text{Fc}^+$  at scan rates of  $50 \text{ mVs}^{-1}$  in THF. The reductions are quasi-reversible and occur at less negative potentials than observed for  $\text{BMes}_3$ .<sup>[17]</sup>

In solution, the compounds are pale yellow with strong absorptions in the 260–314 nm range and weaker absorptions ( $\epsilon < 10000$ ) at higher wavelength assignable to intramolecular charge-transfer transitions; a bathochromic shift is observed as the  $\pi$  system is extended. Compounds **3a** and **3b** emit at 400 and 445 nm and display relatively high quantum yields (Figure 3, Table 1); the quantum yield for **3c** emission at 477 nm drops precipitously. This finding is in keeping with the trend for all-carbon acenes<sup>[18]</sup> and reflects the greater propensity for nonradiative decay paths in more conjugated systems. The optical band gaps, taken from the longest absorption wavelength, also decrease as conjugation

increases. Comparing **3a** to an all-carbon analogue, suberene, it is evident that incorporation of boron influences the photophysics of the molecule by decreasing the gap between the highest occupied and lowest unoccupied molecular orbitals (HOMOs and LUMOs) as well as by lowering the energy of the LUMO. This change results in absorption at longer wavelengths and more intense blue fluorescence in **3a** than in suberene (Table 1). The charge-transfer character of the lowest-energy transitions is indicated by significant solvatochromism effects on the emission wavelength,<sup>[15]</sup> as a result, quantum yields and fluorescence lifetimes are significantly increased in the boron compounds relative to suberene.

DFT calculations<sup>[15]</sup> (RB3LYP 6-31++G (d,p)) on each compound yield planar structures as energy minima when molecular coordinates for the bent solid-state structures are used as input data. Compound **3a** shows HOMOs and LUMOs based on the entire boron–carbon framework (Figure S3 in the Supporting Information), whereas compounds **3b** and **3c** have HOMOs based on the carbon framework and LUMOs with contributions from boron-based orbitals (Figures S4 and S5 in the Supporting Information). However, time-dependent DFT computations show that the major transitions in all of these molecules come from low-lying orbitals based on the annulated carbon system and go to unoccupied orbitals with contributions from boron, in keeping with the observed low-intensity charge-transfer transitions.

In summary, air- and moisture-tolerant analogues of polycyclic aromatic acene hydrocarbons containing a borepin core have been synthesized and characterized. In the solid state they display edge-to-face and face-to-face interactions, and in solution they exhibit blue fluorescence, displaying in some cases high quantum yields.

### Experimental Section<sup>[15]</sup>

**Synthesis of 3a:**  $\text{BCl}_3$  gas (510 mg, 4.35 mmol) was condensed into a solution of **2a** (114 mg, 0.337 mmol) in toluene (90 mL) at  $-78^\circ\text{C}$ . The reaction mixture turned from clear and colorless to light brown. After 80 min, the reaction was warmed to room temperature and concentrated to a total volume of 15 mL. In argon atmosphere, a solution of mesityl lithium (238 mg, 1.89 mmol) in toluene (3 mL) was added dropwise, and the reaction mixture turned yellow. After 16 h, the solvent was removed in vacuo and the product was purified by column chromatography ( $\text{SiO}_2$ , hexanes—25% EtOAc/hexanes—EtOAc). This solid was then recrystallized by slow evaporation of toluene and washed with hexanes to yield **3a** (60 mg, 58%) as large yellow-brownish plates.  $^1\text{H}$  NMR ( $\text{CDCl}_3$ ):  $\delta = 8.06$  (dd,  $J_{\text{HH}} = 7.2$ , 1.2 Hz, 2H), 7.83 (dd,  $J_{\text{HH}} = 7.2$ , 0.8 Hz, 2H), 7.73 (dd dd,  $J_{\text{HH}} = 7.6$ , 1.2 Hz, 2H), 7.43 (dd dd,  $J_{\text{HH}} = 7.2$ , 1.2 Hz, 2H), 7.37 (s, 2H), 6.96 (s, 2H), 2.44 (s, 3H), 1.53 ppm (s, 6H);  $^{13}\text{C}\{^1\text{H}\}$  NMR ( $\text{CDCl}_3$ ):  $\delta = 144.1$ , 141.4, 137.8, 136.2, 134.0, 132.9, 132.7, 127.2, 127.0, 22.9, 21.3 ppm (two peaks for carbon atoms bonded to the boron atom were not observed owing to quadrupolar relaxation).  $^{11}\text{B}$  NMR ( $\text{CDCl}_3$ ):  $\delta = 64.3$  ppm. HRMS calcd for  $\text{C}_{23}\text{H}_{21}\text{B}$ : 308.1736; found: 308.1733. Elemental analysis (%) calcd for  $\text{C}_{23}\text{H}_{21}\text{B}$ : C 89.63, H 6.87; found: C 89.26, H 7.25.

Received: May 25, 2009

Revised: June 15, 2009

Published online: July 13, 2009

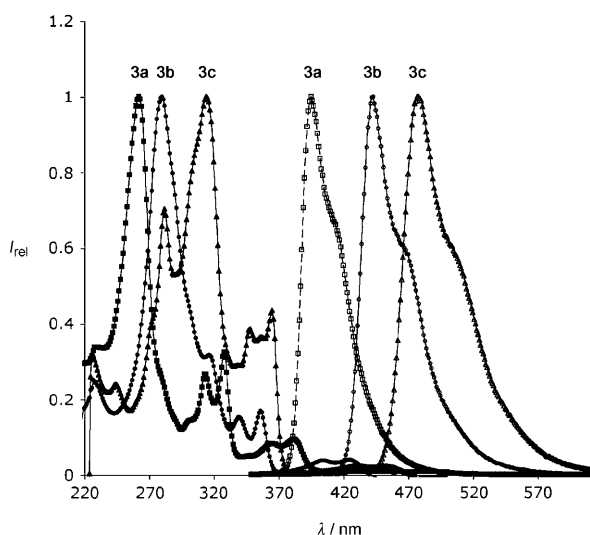


**Figure 3.** Normalized UV/Vis absorbance spectra (solid shapes) and emission spectra (open shapes) for **3a** (squares), **3b** (circles) and **3c** (triangles); dichloromethane,  $2.25 \times 10^{-5} \text{ M}$ .

**Table 1:** Summary of optical data for **3a–c** and hydrocarbon analogue suberene.<sup>[a]</sup>

Compound	Abs $\lambda_{\text{max}}$ [nm]	Em $\lambda_{\text{max}}$ [nm]	$\Phi$ , <sup>[b]</sup> $\tau$ [ns]	Optical BG [eV] <sup>[c]</sup>
<b>3a</b>	260	400	0.70, 11	3.11
<b>3b</b>	280	445	0.39, 13	2.81
<b>3c</b> <sup>[d]</sup>	314	477	0.01, 24	2.61
Suberene	285	384	0.02, 3.6	3.67

[a] see Table S1 in the Supporting Information for a full listing of absorbance bands and extinction coefficients. [b] Absolute quantum yields measured with an integrating sphere. [c] Optical band gap estimated from the onset of absorption in  $\text{CH}_2\text{Cl}_2$  ( $2.25 \times 10^{-5} \text{ M}$ ). [d] Measured in  $\text{CH}_2\text{Cl}_2$  ( $5.0 \times 10^{-5} \text{ M}$ ).

**Keywords:** borepins · boron · fluorescence · heteroacenes · heterocycles

- [1] a) C. D. Entwistle, T. B. Marder, *Angew. Chem.* **2002**, *114*, 3051; *Angew. Chem. Int. Ed.* **2002**, *41*, 2927; b) C. D. Entwistle, T. B. Marder, *Chem. Mater.* **2004**, *16*, 4574; c) F. Jäcke, *Coord. Chem. Rev.* **2006**, *250*, 1107.
- [2] a) A. D. Allen, T. T. Tidwell, *Chem. Rev.* **2001**, *101*, 1333; b) H. Braunschweig, I. Fernandez, G. Frenking, T. Kupfer, *Angew. Chem.* **2008**, *120*, 1977; *Angew. Chem. Int. Ed.* **2008**, *47*, 1951; c) C.-W. So, D. Watanabe, A. Wakamiya, S. Yamaguchi, *Organometallics* **2008**, *27*, 3496.
- [3] a) G. E. Herberich, H. Ohst, *Adv. Organomet. Chem.* **1986**, *25*, 199; b) G. C. Fu, *Adv. Organomet. Chem.* **2001**, *47*, 101.
- [4] a) G. C. Fu, *J. Org. Chem.* **2004**, *69*, 3245; b) G. C. Fu, *Adv. Organomet. Chem.* **2001**, *47*, 101; c) J. C. Rogers, X. Bu, G. C. Bazan, *Organometallics* **2000**, *19*, 3948; d) J. C. Rogers, X. Bu, G. C. Bazan, *J. Am. Chem. Soc.* **2000**, *122*, 730; e) Z. J. A. Komon, J. C. Rogers, X. Bu, G. C. Bazan, *Organometallics* **2000**, *19*, 3948.
- [5] a) A. Wakamiya, K. Mishima, K. Ekawa, S. Yamaguchi, *Chem. Commun.* **2008**, 579; b) S. Yamaguchi, A. Wakamiya, *Pure Appl. Chem.* **2006**, *78*, 1413; c) S. Yamaguchi, T. Shirasaka, S. Akiyama, K. Tamao, *J. Am. Chem. Soc.* **2002**, *124*, 8816; d) S. Kim, K. Song, S. O. Kang, J. Ko, *Chem. Commun.* **2004**, 68; e) K. S. Thanthiriatte, S. R. Gwaltney, *J. Phys. Chem. A* **2006**, *110*, 2434.
- [6] a) J. M. Schulman, R. L. Disch, M. L. Sabio, *J. Am. Chem. Soc.* **1982**, *104*, 3785; b) R. L. Disch, M. L. Sabio, J. M. Schulman, *Tetrahedron Lett.* **1983**, *24*, 1863; c) G. Subramanian, P. von R. Schleyer, H. Jiao, *Organometallics* **1997**, *16*, 2362.
- [7] J. J. Eisch, J. E. Galle, B. Shafii, A. L. Rheingold, *Organometallics* **1990**, *9*, 2342.
- [8] a) E. E. van Tamelen, G. Brieger, K. G. Untch, *Tetrahedron Lett.* **1960**, *1*, 14; b) A. J. Ashe III, W. Klein, R. Rousseau, *Organometallics* **1993**, *12*, 3225; c) A. Jingui, R. Nakazawa, T. Yagi, I. Murata, *Tetrahedron* **1994**, *50*, 6495; d) Y. Sugihara, R. Miyatake, I. Murata, A. Imamura, *J. Chem. Soc. Chem. Commun.* **1995**, 1249; e) H. Sashida, A. Kuroda, T. Tsuchiya, *Chem. Commun.* **1998**, 767; f) H. Sashida, A. Kuroda, *J. Chem. Soc. Perkin Trans. 1* **2000**, 1965.
- [9] J. M. Schulman, R. L. Disch, *Organometallics* **2000**, *19*, 2932.
- [10] T. K. Wood, W. E. Piers, B. A. Keay, M. Parvez, *Angew. Chem.* **2009**, *121*, 4069; *Angew. Chem. Int. Ed.* **2009**, *48*, 4009.
- [11] a) J. E. Anthony, *Angew. Chem.* **2008**, *120*, 460; *Angew. Chem. Int. Ed.* **2008**, *47*, 452; b) J. E. Anthony, *Chem. Rev.* **2006**, *106*, 5028; c) M. Bendikov, F. Wudl, D. F. Perepichka, *Chem. Rev.* **2004**, *104*, 4891.
- [12] a) T. R. Kelly, Q. Li, V. Bhushan, *Tetrahedron Lett.* **1990**, *31*, 161; b) D. C. Harrowven, I. L. Guy, M. Howell, G. Packham, *Synlett* **2006**, 2977; c) J.-L. Zhang, P. W. H. Chan, C.-M. Che, *Tetrahedron Lett.* **2003**, *44*, 8733.
- [13] a) T. Agou, J. Kobayashi, T. Kawashima, *Chem. Commun.* **2007**, 3204; b) T. Agou, J. Kobayashi, T. Kawashima, *Chem. Eur. J.* **2007**, *13*, 8051.
- [14] J. D. Kennedy in *Multinuclear NMR* (Ed. J. Mason), Plenum, New York, **1987**, chap. 8.
- [15] See Supporting Information for full details.
- [16] Crystal data for **3a**: C<sub>23</sub>H<sub>21</sub>B, *M<sub>r</sub>* = 308.21, monoclinic, *P*<sub>2</sub><sub>1</sub>/*n*, *a* = 9.408(6), *b* = 8.469(5), *c* = 22.011(12) Å, *β* = 93.56(2)°, *V* = 1750.4(18) Å<sup>3</sup>, *Z* = 4, *ρ* = 1.170 g cm<sup>-3</sup>, MoK<sub>α</sub> radiation, *λ* = 0.71073 Å, *T* = 173(2) K, 7463 measured reflections, 3940 unique, min/max transmission = 0.9820 and 0.9846, *R*<sub>1</sub> (*I* > 2σ) = 0.0554, *wR*<sub>2</sub> = 0.1308, *GoF* = 1.041, No. of parameters = 217, final difference map within +0.272 and -0.201 e Å<sup>-3</sup>. Crystal data for **3b**: C<sub>27</sub>H<sub>23</sub>B, *M<sub>r</sub>* = 358.26, monoclinic, *C*<sub>2</sub><sub>1</sub>/*c*, *a* = 34.623(7), *b* = 7.992(3), *c* = 15.450(5) Å, *β* = 113.71(3)°, *V* = 3914(2) Å<sup>3</sup>, *Z* = 8, *ρ* = 1.216 g cm<sup>-3</sup>, MoK<sub>α</sub> radiation, *λ* = 0.71073 Å, *T* = 173(2) K, 6081 measured reflection, 3567 unique, min/max transmission = 0.9953 and 0.9886, *R*<sub>1</sub> (*I* > 2σ) = 0.0510, *wR*<sub>2</sub> = 0.1117, *GoF* = 1.040, No. of parameters = 254, final difference map within +0.214 and -0.227 e Å<sup>-3</sup>. Crystal data for **3c**: C<sub>31</sub>H<sub>25</sub>B, *M<sub>r</sub>* = 408.32, monoclinic, *P*<sub>2</sub><sub>1</sub>/*n*, *a* = 11.642(3), *b* = 8.660(4), *c* = 22.879(7) Å, *β* = 103.90(2)°, *V* = 2239.1(14) Å<sup>3</sup>, *Z* = 4, *ρ* = 1.211 g cm<sup>-3</sup>, MoK<sub>α</sub> radiation, *λ* = 0.71073 Å, *T* = 173(2) K, 8599 measured reflection, 5039 unique, min/max transmission = 0.9893 and 0.9906, *R*<sub>1</sub> (*I* > 2σ) = 0.0671, *wR*<sub>2</sub> = 0.1393, *GoF* = 1.081, No. of parameters = 289, final difference map within +0.325 and -0.250 e Å<sup>-3</sup>. CCDC 730729 (**3a**), 730730 (**3b**), and 730731 (**3c**) contain the supplementary crystallographic data for this paper (excluding structure factors). These data can be obtained free of charge from The Cambridge Crystallographic Data Centre via www.ccdc.cam.ac.uk/data\_request/cif.
- [17] S. A. Cummings, M. Iimura, C. J. Harlan, R. J. Kwaan, I. Vu Trieu, J. R. Norton, B. M. Bridgewater, F. Jäcke, A. Sundaraman, M. Tilset, *Organometallics* **2006**, *25*, 1565.
- [18] M. Montalti, A. Credi, L. Prodi, M. T. Gandolfi, *Handbook of Photochemistry*, 3rd ed., CRC/Taylor & Francis, **2006**, pp. 86–156.